Research Article

Chemical Review and Letters
journal homepage: www.chemrevlett.com
ISSN (online): 2645-4947 (print) 2676-7279

Synthesis, spectroscopic and computational investigation of bis (3 methoxyphenylthio) ethyl) naphthalene

Farnaz Behmagham [a, *], Zahra Asadi [b], Yahya Jamale Sadeghi [c]

[a] *Department of Chemistry, Miandoab Branch, Islamic Azad University, Miandoab, Iran*
[b] *Department of Chemistry, Miyaneh Branch, Islamic Azad University, Miyaneh, Iran*
[c] *Department of Chemistry, Payame Noor University, Tehran, Iran*

ARTICLE INFO

Article history:
Received 18 November 2018
Received in revised form 1 December 2018
Accepted 5 December 2018
Available online 5 December 2018

Keywords:
Bis(3-methoxyphenylthio)ethyl)naphthalene
Cleavage reaction of epoxide rings
Organosilicon
RM06-2X
PBE1PBE
FT-IR
NMR

ABSTRACT

In this study, we report an interesting combined experimental and theoretical studies on the molecular structure of 2-(2,2-bis(3-methoxyphenylthio)ethyl)naphthalene (**5**). The compound **5** was unexpectedly synthesized and characterized by FT-IR, ^{1}H NMR, ^{13}C NMR, mass spectrum, and elemental analyses. The optimized geometry and mulliken charge density on atoms of **5** were calculated by RM062X and PBE1PBE methods using a 6-31+G(d) basis set. The experimental obtained IR spectra of **5** was compared to the theoretical results at the RM062X/PBE1PBE/6-31+G(d) level which explained in terms of potential energy distribution (PED) analysis. The scaled theoretical vibrational wavenumber displayed very good agreement with experimental data. The calculated proton and carbon chemical shifts show almost a nice correlation with experimental data using RM062X/6-31+G(d) level. Theoretical investigations of frontier molecular orbitals, mapped molecular electrostatic potential (MEP), thermodynamic properties and physico-chemical characteristics of **5**, were also acquired.

1. Introduction

2,2-Bis(trimethylsilyl)oxirans are very significant compounds that used to production of organosilicon compounds [1,2]. Cleavage reaction of epoxide rings with thiols is very beneficial in pharmaceutical and natural product chemistry [3]. Commonly, thiolysis of epoxides can be performed by a base [4] or a Lewis acid [5], or in the existence of a heterogeneous catalysts [6]. Ring opening reactions of epoxides having organosilicon group with the attack of the nucleophiles has been extensively investigated [7-9]. These compounds react with various types of reactants *via* cleavage reaction of epoxide ring. The cleavage reaction of epoxide ring in alkyl silicon compounds has generally led to produce 1-trimethylsilylvinyl sulfides, **3**, as a major product and 1-bromovinyl silane, **4**, as a minor product through reaction between (3-(naphthalen-2-yl)-2,2-bis(trimethylsilyl) oxiran, **2**, with ArSH/$MgBr_2$ (Scheme 1). In this study, however, cleavage reaction of (3-(naphthalene-2-yl)-2,2-bis(trimethylsilyl) oxiran, **2**, surprisingly produces **5** as a major product and 1-bromovinyl silane, **4**, as a minor product in the presence of magnesium bromide catalyst and 3-methoxythio phenol (Scheme 2). In this study, we proposed an interesting mechanism for the synthesis of **5** (Scheme 3). Also, the structural explanations for **5** such as geometrical optimization is scrutinized using both experimental and theoretical methods including M062X and PBE1PBE methods using 6-31+G(d) basis set. Vibrational wavenumber, proton and carbon NMR chemical shifts, energy gaps and HOMO-LUMO orbitals were performed with same methods using 6-31+G(d) basis set.

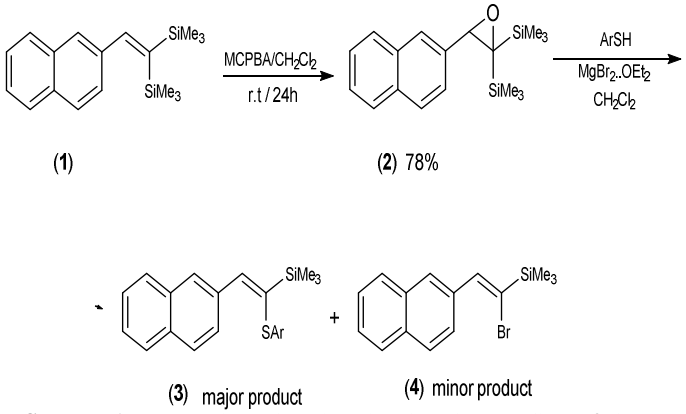

Scheme 1. Preparation of 1-trimethylsilylvinyl sulfides, **3**, in major product and 1-bromovinyl silane, **4,** in minor product.

2. Experimental

2.1 General method

The reaction was performed under dry argon. Solvents were dried by standard methods. Substrates for the synthesis of (3-(naphthalene-2-yl)-2,2-bis(trimethylsilyl)oxiran, **2**, are 2-naphthaldehyde (Merck) and MCPBA (Acros). Products were characterized by IR, ^{1}H NMR and ^{13}CNMR spectra, and mass spectral data. IR spectra measured on a Bruker-Tensor 270 spectrometer. Proton and carbon NMR spectra were recorded on Bruker FT-400 MHz instrument in d-chloroform as a solvent. Mass spectra were obtained on GC-mass Agilent quadrupole mode 5973N device, working at 70 eV. The elemental analyses were carried out by using an Elementar Vario EL III device. The synthetic way and reaction mechanism were presented in Schemes 1, 2 and 3.

2.2. Synthesis

*2.2.1. Synthesis of (3-(naphthalene-2-yl)-2,2-bis(trimethylsilyl)oxiran (**2**) [10]*

A mixture of vinylsilane, **1**, (2.00 g, 6.71 mmol) and *m*-chloroperbenzoic acid (MCPBA) (75% w/w pure) stirred in CH_2Cl_2 (80ml) at room temperature for 20h. The mixture was washed with aq. $NaHCO_3$ (4× 30 ml), water (35 ml) and brine (35 ml). The organic phase was dehydrated and dried by $MgSO_4$. Solvent was vaporized and further purification was done by column chromatography (1:4 n-hexane:ethyl acetate) to obtain (3-(naphthalene-2-yl)-2,2-bis(trimethylsilyl)oxiran, **2**, as a yellow liquid.

*2.2.2. Synthesis of 2-(2,2bis (3methoxyphenylthio) ethyl) naphthalene (**5**)*

A mixture of epoxide **2** (0.5 mmol), *m*-methoxythiophenol (1.2 mmol), dry dichloromethane (3-4 ml) and $MgBr_2$ (0.3 mmol) was shaken in a flask. The progress of the reaction was monitored by TLC until the starting material entirely disappeared. The mixture was diluted in dichloromethane (15 ml) and washed twice with water (15 ml). The organic layer was dried over Na_2SO_4 and the solvent was removed at low pressure, and the product was obtained by preparative TLC on silica gel. Analytical data for, **5**, were shown below**:**

Yellowish liquid (40%): (R_f= 0.24 10:1 hexane normal:ethyl acetate), FT-IR (KBr, cm^{-1}): 3054(CH, Aryl), 2956 (CH, Alkyl), 2924 (CH), 1636 and 1470 (C=C, Aryl); ^{1}H NMR(400 MHz, $CDCl_3$): δ 3.33 (d, 2H, J=7.04 Hz, CH_2), 3.71 (s, 6H, OCH_3), 4.71 (t, 1H, J=8 Hz, CH), 6.79-7.80(m, 15H,Ar); ^{13}C NMR ($CDCl_3$): δ 41.52 (CH_2), 54.22 (CH), 58.38 (CH_3), 112.75-158.68 (Ar); m/z (EI): 432 (7%, $[M]^+$), 293 (78%, $[M-SC_6H_4OMe]^+$, 153 (28%, $CH_2SC_6H_4OMe]^+$, 139 (28%, $[SC_6H_4OMe]^+$. Anal. Calc. for $C_{26}H_{24}O_2S_2$: C, 72.2; H, 5.5. Found: C, 72.4; H, 5.8%. We previously mentioned that 1-trimethylsilylvinyl sulfides, **3**, and 1-bromovinyl silane, **4**, were generally produced through cleavage reaction of epoxide ring in alkylsilicon, **2**, *via* attack of ArSH/$MgBr_2$ (Scheme 1). In this study, however, cleavage reaction of (3-(naphthalene-2-yl)-2,2-bis(trimethylsilyl) oxiran, **2**, surprisingly produces **5** as a major product and 1-bromovinyl silane, **4**, as a minor product in the presence of magnesium bromide catalyst and excess 3-methoxythiophenol (Scheme 2).

The difference of this reaction which makes it to obtain different product of **5** is using excess 3-methoxythiophenol.

The proposed mechanism was explained in synthesis of **5** (Scheme 3). 3-Methoxythiophenol was added to 2,2-bis(trimethylsilyl)oxiran, 2, to produce a salt bis(trimethylsilyl) thioether, **6**. The trimethylsiloxy salt, BrMgOSiMe3, was removed to produce vinylsilane, **3**. The compound **3** could be converted to a three-membered ring sulfonium methylide, **7**. Sulfonium methylide, **7**, could be protonated to formation of the thiiranium cation **8** which converted to a carbocation **9**. A hydride shift occurs on the carbocation **9** to produce a more stable carbocation **10** which forms the trimethylsilyl derivative **11** through reaction with 3-methoxythiophenol. Trimethylsilyl derivative **11** undergoes a reaction with bromide ion to produce compound **5**.

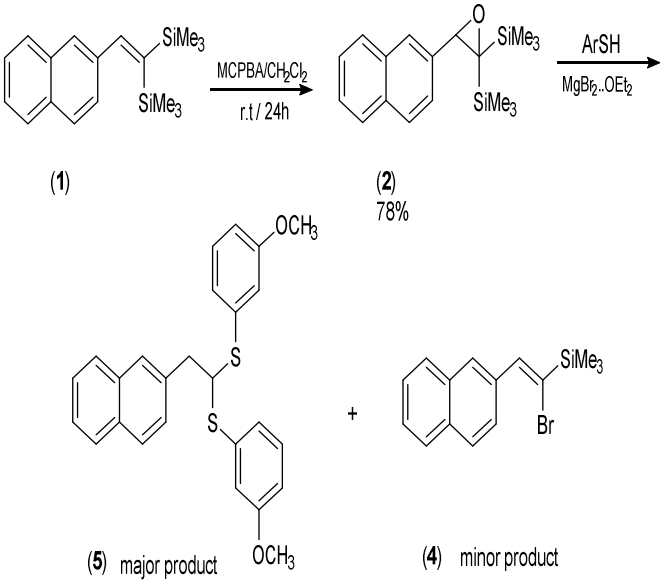

Scheme 2. Preparation of unexpected bis(3-methoxyphenylthio) ethyl naphthalene, **5**, in major product and 1-bromovinyl silane, **4,** in minor product.

3. Computational details

In this study, the quantum chemical computations were performed at the DFT levels by the Gaussian 03 program [11]. The geometries were fully optimized and then frequency calculations were done using M062X and PBE1PBE methods. The gauge-independent atomic orbital (GIAO) technique was applied for the proton and carbon chemical shifts in **5** [12].

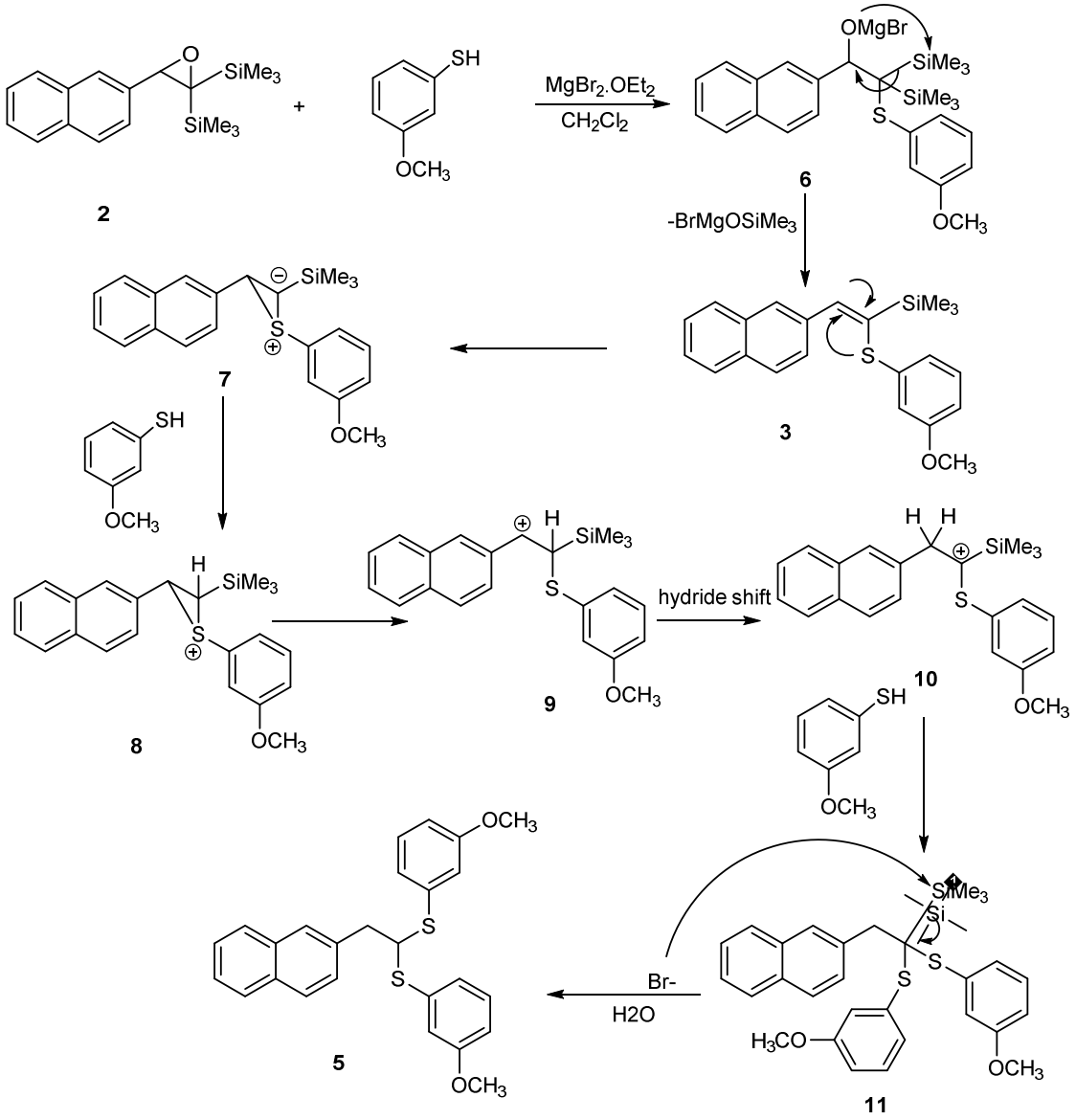

Scheme. 3. The proposed mechanism for synthesis of 2-(2,2-bis(3-methoxyphenylthio) ethyl)naphthalene (**5**)

The calculated isotopic amount of the shielding tensor σ_{cal} were scaled from that of TMS: $\delta = \sigma_{TMS} - \sigma_{cal}$ (ppm), for calculating the ^{1}H and ^{13}C chemical shifts (δ) in **5**. In addition, simulating the ^{1}H and ^{13}C chemical shifts of compound were done by GaussView software [13]. The plots of density of states (DOS) were achieved using the GaussSum program [14]. Thermodynamic and physico-chemical properties of this structure were also investigated.

4. Results and Discussion

4.1. Geometrical structures and atomic charge

The global optimized structure of **5** is presented in Fig. 1. The calculated bond lengths at the RM06/2X and PBE1PBE levels of theory listed in Table 5S in Supplementary section. The product of **5** was obtained as a yellowish liquid. Therefore, we can not obtain the X-Ray spectrum of **5** and we have to use the analogue compounds for comparison of the theoretical results [Fig 1S-4S]. The corresponding experimental information is presented for comparison in Table 5S [15-17].

The investigation of the data shown in Table 5S reveals that the obtained bond lengths at the RM06/2X and PBE1PBE levels are independent of the method and basis set used. Fig. 2 indicates the correlations between the experimental and calculated bond lengths. Obviously, a good linear correlation is achieved between the RM062X/6-31+G(d) and PBE1PBE/6-31+G(d) levels *vs.* experimental data. The calculated bond angles and dihedral angles and corresponding experimental data [15-17] are collected in Tables 6S and 7S. It was found that obtained data for bond angles and

dihedral angles of **5** using the RM062X method are as the same as the PBE1PBE method.

The obtained Mulliken atomic charges of **5** at the M062X and PBE1PBE levels are shown in Table 8S.

The calculated Mulliken atomic charges on atoms in this molecule indicated that the great amount of positive charge is placed on the C3 atom, +0.796 and +0.993 at the M062X and PBE1PBE levels, respectively. The carbon C21 have the most negative charge -1.519 and -0.829 at the M06-2X and PBE1PBE levels, respectively (Fig. 1).

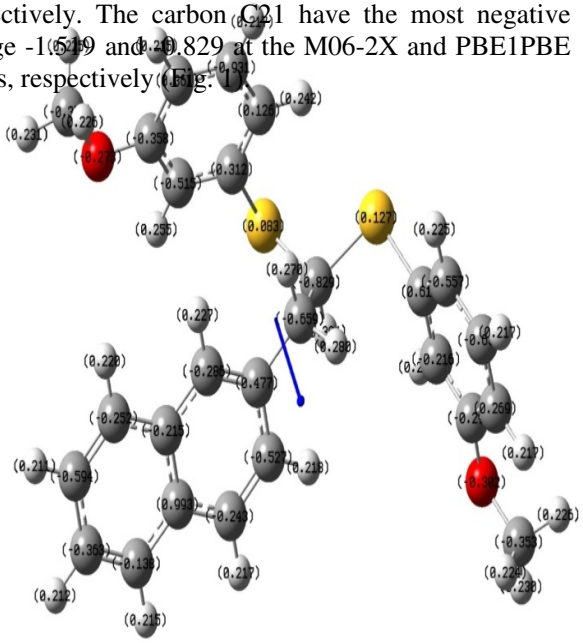

Fig. 1. The optimized structure and the charges on atoms of **5** calculated at the RPBE1PBE/6-31+G(d) level.

4.2. Vibrational assignments

The experimental and theoretical IR spectra of **5** are demonstrated in Fig. 3 and Table 1S. Theoretical calculations are indicated that the mentioned structure has the C1 point group symmetry with 54 atoms.

The number of vibration normal modes of **5** is 155 normal vibrational modes, 103 modes of vibrations are in-plane and 51 modes are out-of-plane. The bands that are in the plane of the molecule are illustrated as A', while out of the plane bands are dedicated as A". So, the 139 normal modes of vibrations of **5** are divided as Γ_{vib}= 103A' +52A". Table 1S shows the experimental and scaled and unscaled theoretical frequencies and infrared intensities of **5** which computed at the RM062X and PBE1PBE methods. The RM062X and PBE1PBE methods explained relationship between the experimental and computed frequencies of 5. Fig. 4 indicated that the results acquired by RM062X (R^2=0.9998) and PBE1PBE (R^2 =0.9996) methods are in good agreement with the experimental values.

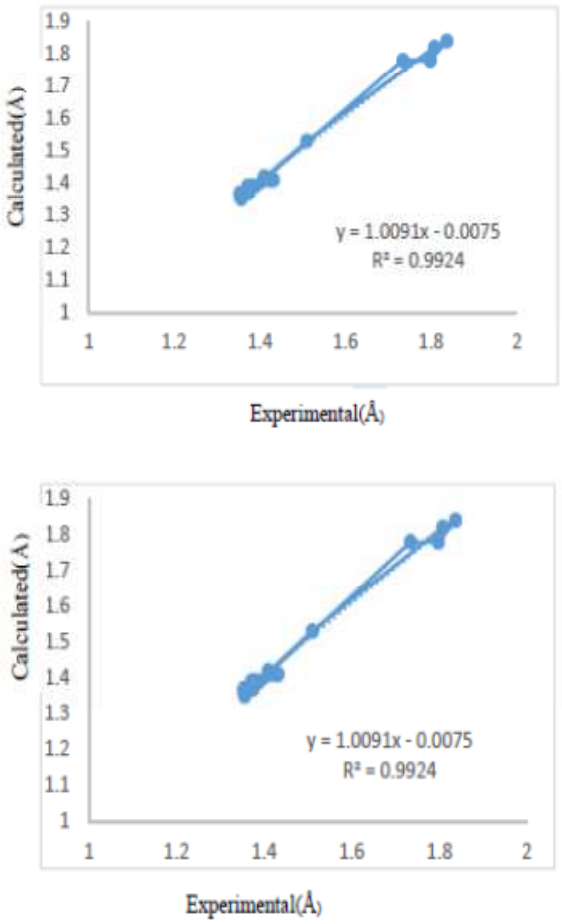

Fig. 2. The bond length correlations between the experimental and calculated data for **5**.

4.2.1. C-S vibrations

The C-S bond in aromatic is assigned in the region of 570-710 cm-1 [19]. In this structure, the C-S bond is seen at 740 cm^{-1}.

The calculated C-S stretching vibration appears at 770.78 cm^{-1} using the RM062X/6-31+G (d) level which was closer to experimental data. The calculated C-S stretching vibrations appear at 765.06 cm^{-1} by the PBE1PBE /6-31+G(d) level.

This mode (mode no. 99) involves the contribution of 23%, as indicated by the PED.

4.2.2. C-O vibrations

The C-O bond in aromatic is assigned in the region of 1000-1300 cm^{-1}. In this structure, the C-O bond is obtained at 1039 cm^{-1}.

The calculated C-O stretching vibration appears at 1068.04 cm^{-1} using the RM062X/6-31+G (d) level

which was closer to experimental data. The calculated C-O stretching vibrations appear at 1058.5 cm^{-1} by the PBE1PBE /6-31+G(d) level. This mode (mode no. 74) involves the contribution of 59%, as indicated by the PED.

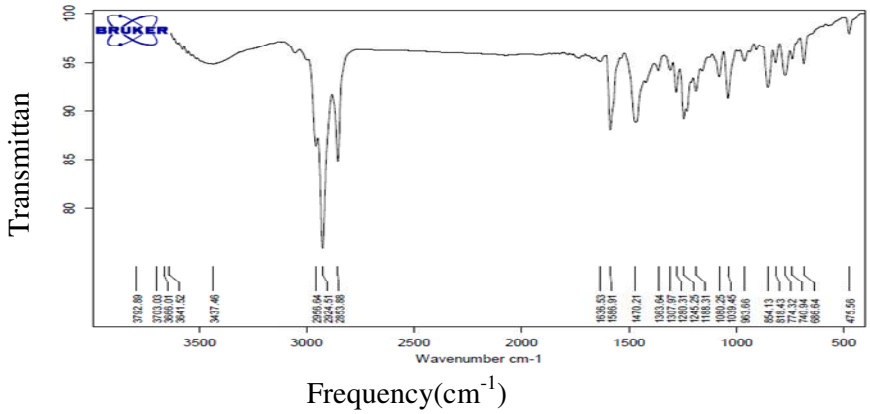

ed IR spectra for **5**.

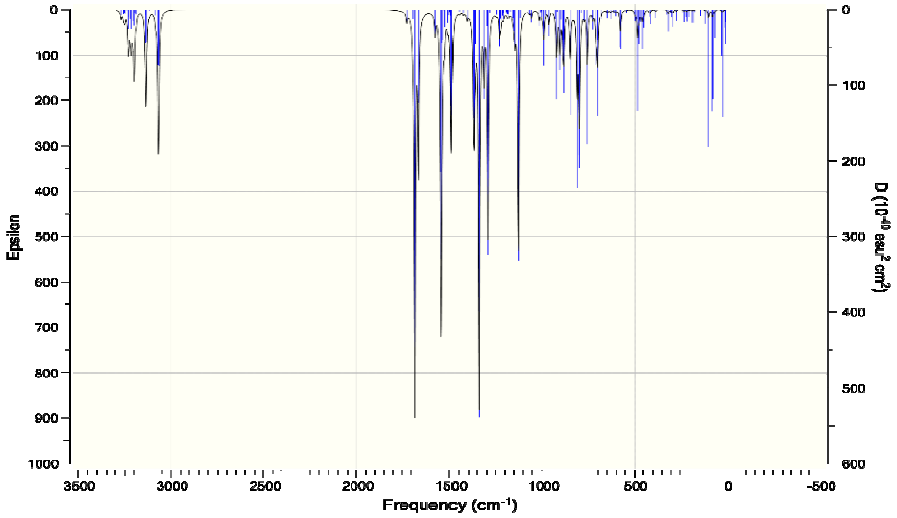

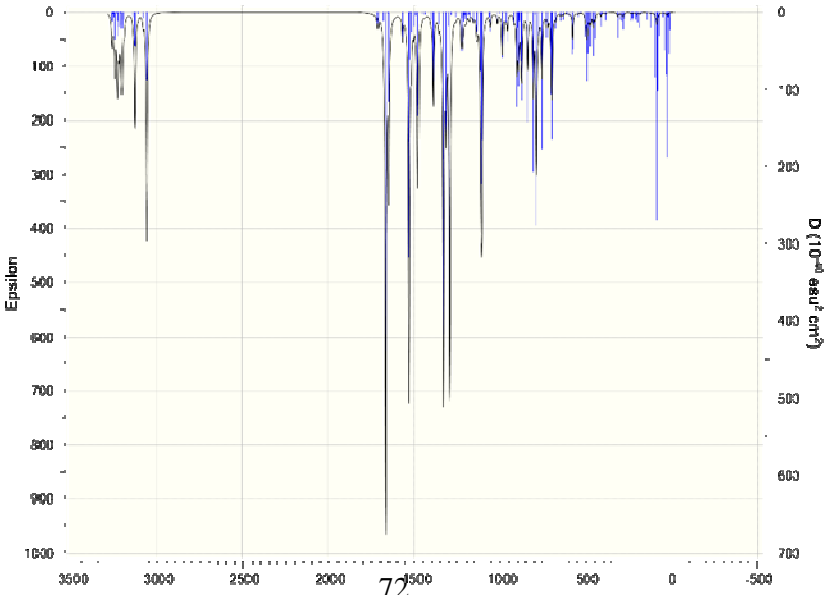

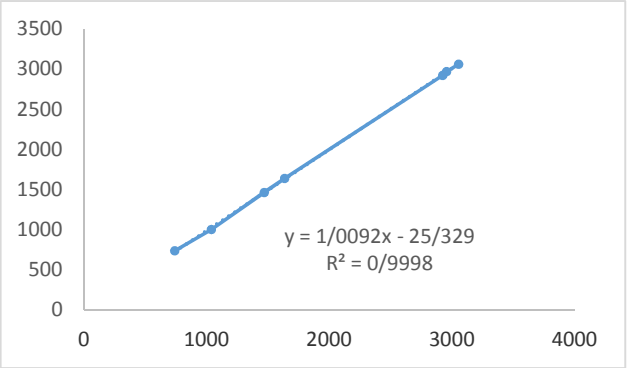

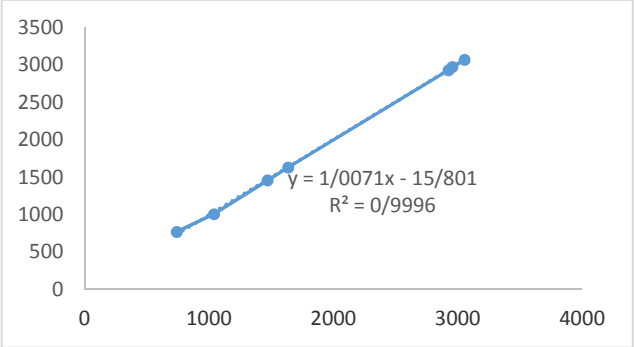

Fig. 4. Relationship between the experimental and computed frequencies of **5**.

4.2.3. C–H vibrations

The regions of 2850-3000 cm^{-1} and 3000–3100cm^{-1} are related to the C–H stretching vibration in alkanes and aromatic structures, respectively [11, 12]. The C–H stretching vibrations in IR bands appeared at 3054, 2956 and 2924 cm^{-1}. The computed C–H stretching vibrations observed at 3056.45, 2964.79 and 2916.75 cm^{-1} applying the RM062X/6-31+G(d) level that show very good correlation with experimental results. The calculated C–H stretching vibrations obtained at 3064.89, 2969.56 and 2924.66 cm^{-1} using the PBE1PBE /6-31+G(d) level.

This mode (modes no. 8, 20 and 22) involves the contribution of 84, 100, and 100% respectively, as evidenced by the PED analysis.

4.2.4. C=C vibrations

The region of 1400-1600 cm^{-1} is belonged to the C=C bond in aromatic compounds [18]. For this compound, the C=C bond is observed at 1636 cm^{-1}. The computed C=C stretching vibration appears at 1635.78 cm^{-1} using the RM062X/6-31+G (d) level that was mostly close to experimental data. The calculated C=C stretching vibrations by the PBE1PBE /6-31+G(d) level appear at 1625.96 cm^{-1}.

This mode (mode no. 25) involves the contribution of 62%, as demonstrated by the PED analysis.

4.2.5. C-H bending vibrations

The C-H bending absorption observed in the region of 1350-1480 cm^{-1} [19]. This structure showed the C-H bending at 1470 cm^{-1}.

The computed C-H bending vibration appears at 1460.52 cm^{-1} using the M06-2X/6-31+G (d) level which was close to experimental data. The calculated C-H bending vibrations appear at 1453.91 cm^{-1} by the PBE1PBE/6-31+G(d) level.

As illustrated by the PED, this mode (mode no. 33) associated to the contribution of 44%.

4.3. Chemical shift analysis

4.3.1. Proton chemical shift analysis, ^{1}H NMR

Fig. 5 displays experimental and theoretical simulation of ^{1}H and ^{13}C NMR spectra which were accomplished by GaussView software. The experimental and theoretical chemical shifts of protons for **5** are listed in Table 2S. It is found that the ^{1}H chemical shift values (with respect to TMS) observe at 3.13–9.25 ppm and 3.07–8.64 ppm by M062X and PBE1PBE levels, respectively, whereas the experimental proton shifts are in the range of 3.33–7.80 ppm. The methoxy protons (H48, H49, H 50 and H52, H53, H54) experimentally resonate at 3.71ppm as a multiplet which these chemical shifts are theoretically predicted in the range of 3.32–4.88 ppm and 4.24–4.90 at M062X and PBE1PBE levels, respectively. The signal in 3.33 ppm was related to methylene protons (H19 and H20) which these chemical shifts are theoretically predicted in the range of 3.13–3.17 ppm and 3.07 –3.36 at M062X and PBE1PBE levels, respectively. The CH proton (H22) of **5** are experimentally assigned at 4.71 ppm. This chemical shift theoretically occurs at 5.26 and 5.41ppm by M062X and PBE1PBE levels of theory. The multiplet at 6.79–7.80 ppm correlated with the aromatic protons (H44, 34, 16, 29, 39, 17, 43, 8,41, 33, 13, 7,9, 12, 31) that are theoretically obtained at 7.53–9.25 and 7.16–8.64 ppm by M062X and PBE1PBE, respectively.

4.3.2. Carbon chemical shift analysis, ^{13}C NMR

As Table 3S shows the ^{13}C chemical shifts (with respect to TMS) are obtained in the range of 171.36–43.83 and 155.2–42.66 ppm by M062X and PBE1PBE levels, respectively, while the corresponding experimental results are detected in the range of

41.52–158.68 ppm. The largest deviation between the calculated and experimental ^{13}C NMR chemical shifts ($|\delta_{exp}-\delta_{M062X}|$) is belong to C21 (-18.26) using M062X level and C5 (19.38) ppm using PBE1PBE level. The chemical shifts of C18, C21, C51, and C32 are experimentally assigned in the 41.52, 54.22, 58.38 and 112.75 ppm, respectively. The theoretical chemical shift values of these atoms dedicated at 43.83 (error approx. -2.31 ppm), 72.48 (error approx. -18.26ppm), 57.56 (error approx. 0.82 ppm) and 120.58 (error approx. -7.83ppm) at M06-2X, and 42.66 (error approx. -1.14 ppm), 66.53

(error approx. -12.31 ppm), 56.42 ppm (error approx. 1.96 ppm) and 106.67 ppm (error approx. 6.08 ppm) at the PBE1PBE level. Full data of ^{13}C NMR chemical shifts were presented in Table 3S.

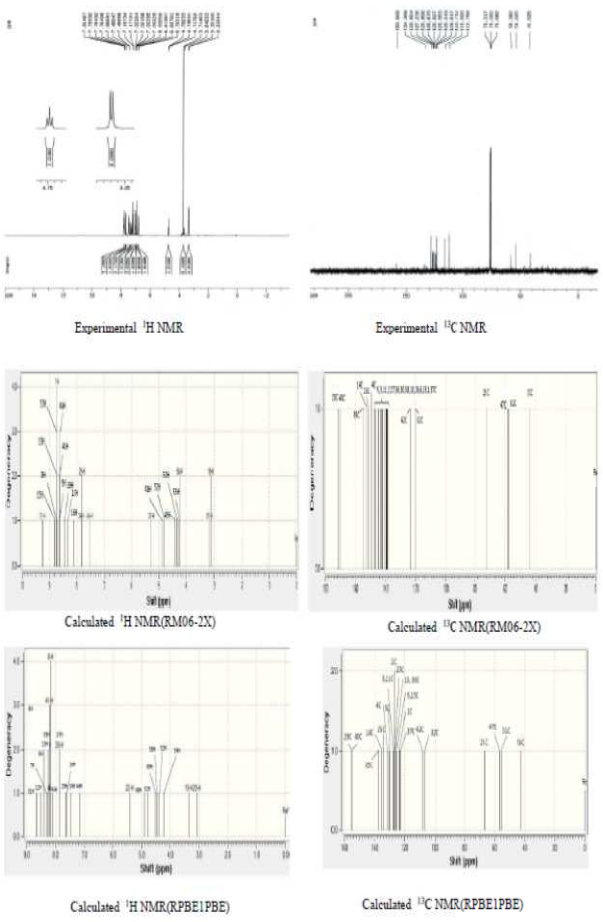

Fig. 5. Experimental and calculated ^{1}H NMR and ^{13}C NMR spectra.

The correspondence between the experimental and computed chemical shifts of ^{1}H and ^{13}C NMR is illustrated in Fig. 6. Obviously, the relationship between the experimental and theoretical chemical shifts is better for ^{13}C atoms more than for ^{1}H atoms. This difference can be anticipated because the ^{1}H chemical shifts were more sensitive to solvent effects [20].

As seen in Fig. 7, the M062X data (R^2_{HNMR} =0.9764 and R^2_{CNMR} =0.9862) were found be closer to the experimental values in contrast with PBE1PBE values (R^2_{HNMR}=0.9555 and R^2_{CNMR} =0.9797).

4.4. Frontier molecular orbital analysis

The GaussSum program was applied to give the molecular orbital data to obtain density of states (DOS) diagram [14].

The DOS diagram for **5** is demonstrated in Fig. 7. The DOS diagram mostly provided the collection of the fragment orbitals are partnership in molecular orbitals.

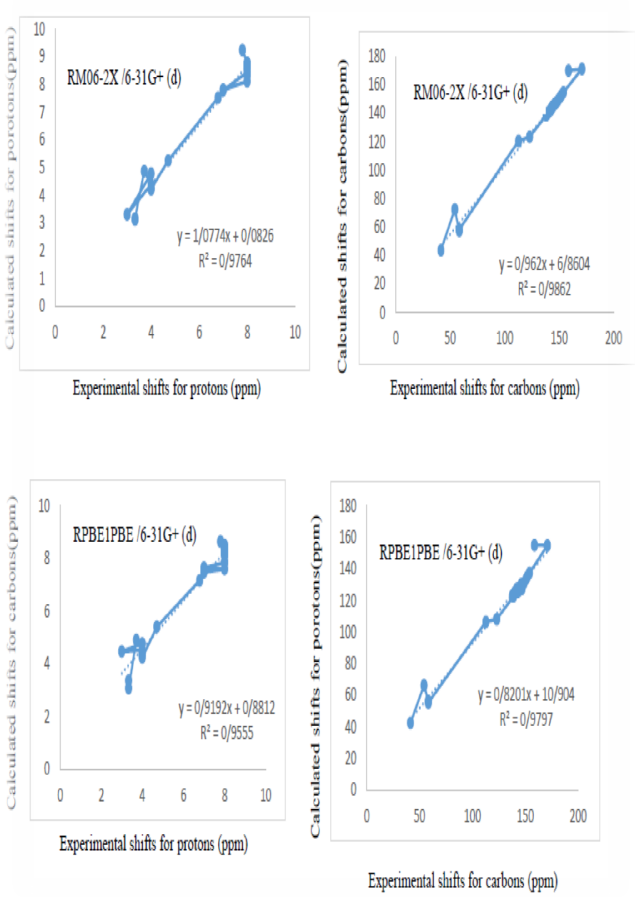

Fig. 6. Relationship between the experimental and computed chemical shift for ^{1}H and ^{13}C NMR of **5**.

The HOMO-LUMO energy gap is energy difference between the highest occupied molecular orbital (HOMO) and lowest unoccupied molecular orbital (LUMO) which explains the chemical activity of the molecule. These data can be employed as a simple guide of kinetic stability. It is noticeable that the high amounts of energy differences lead to the higher kinetic stability. The calculated energy gap of **5** at PBE1PBE/6-31+G (d) and M06-2X/6-31G+(d) levels are 5.004 and 6.678 eV, respectively. This result shows that electron-correlation effects tend to reduce the HOMO-LUMO energy gap of **5**. So, for this molecule at the PBE1PBE level, less kinetic stability is predicted.

4.5. Molecular electrostatic potential map

The molecular electrostatic potential (MEP) is a reactivity map representing most possible areas for the nucleophilic sites which electrophile reagents can attack on those sites [20]. The MEP map of **5** is shown in Fig. 8. Blue colors show positive MEP regions, while red colors illustrate negative MEP regions. The MEP map of **5** are in the range from -0.156 to +0.157 au.

This picture exhibits that the C28-O46 bond have more negative MEP region in compared with other atoms. It irealized that that oxygen atom can tolerate the protonation reaction with acidic reagents.

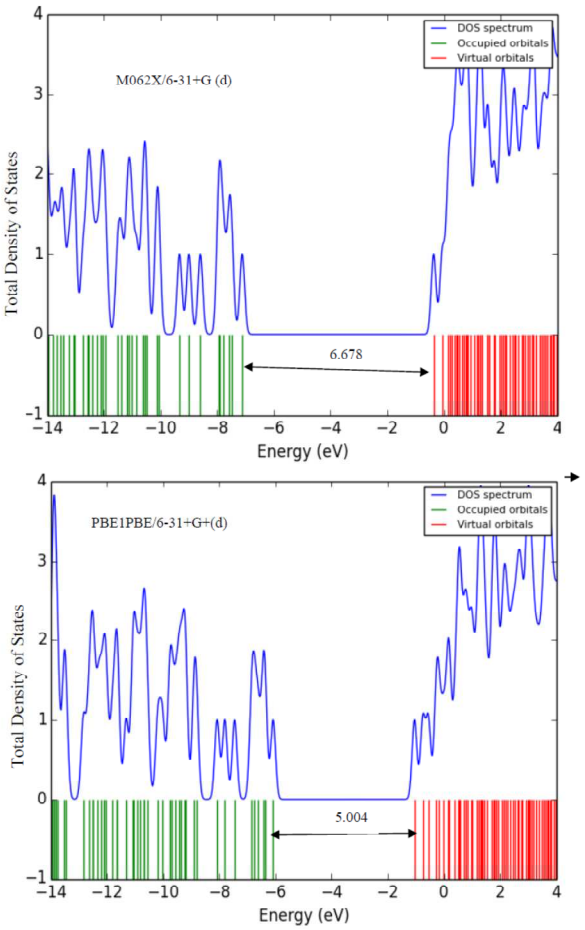

Fig. 7. DOSdiagram contains HOMO(left) and LUMO(right) plot of **5** at M062X and PBE1PBE methods with /6-31G+(d) basis set.

4.6. Calculated thermodynamic and physico-chemical properties

The thermodynamic properties involving total energies, free Gibbs energies, entropies and some other thermodynamic properties computed for **5** (Table 4S). The logarithm of the partition coefficient (log P values) of **5** was computed in n-octanol/water as solvent mixture using two commercially available programs (ChemBioOffice Ultra 11.0 [22], and ACD/LogP [23]).

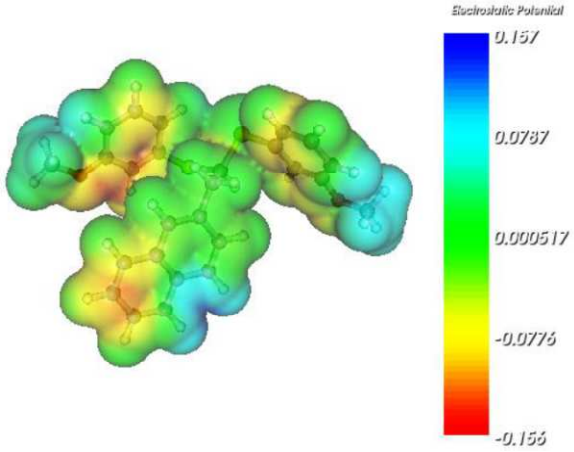

Fig. 8. The molecular electrostatic potential (MEP) of **5**.

5. Conclusions

The compound **5** was synthesized *via* Magnesium bromide catalyzed ring cleavage reaction of (3-(naphthalene-2-yl)-2, 2-bis(trimethylsilyl)oxiran, 2, *via* 3- methoxy thiophenol. The structure of **5** was distinguished and characterized by elemental analysis, FT-IR, ^{1}H and ^{13}C NMR. Comparison between the computed and experimental data demonstrated that the both PBE1PBE and M062X methods with 6-31+G(d) basis set obtained identical data for bond length, bond angle and dihedral angles of **5**. Moreover, it is found that the PBE1PBE/6-31+G(d) M062X calculated vibrational wavenumbers are in good agreement with the experimental IR spectra whereas at ^{1}H and ^{13}C NMR calculation, M062X/6-31+G(d) method are in good agreement with the experimental data. The MEP map of 5 anticipates that the oxygen atom of **5** is the most reactive site to electrophilic attack.

References

[1] D.M. Hodgson, P.J. Comina, A remarkable base-induced rearrangement of epoxydisilanes, Tetrahedron Letters, 31 (1996) 5613–5614.

[2] P. Pawluc, G. Hreczycho, B. Marciniec, A New Selective Approach to 1,1-Bis(silyl)-2-aryl-ethenes and 1,1-Bis(silyl)-1,3-butadienes via Sequemtial Silylative Coupling - Heck Coupling Reactions, J. Org. Chem. 71 (2006) 8676-8679.

[3] M.M. Mojtahedi, M.S. Abaee, M. Bolourchian, H. Abbasi, Facile Room-Temperature MgBr2· OEt2-Catalyzed Thiolysis of Epoxides Under Solvent-Free Conditions, Phosphorus, Sulfur, and Silicon, 182 (2007) 905-910.

[4] (a) C.H. Behrens, K.B. Sharpless, Selective transformations of 2,3-epoxy alcohols and related derivatives. Strategies for nucleophilic attack at carbon-3 or carbon-2, J. Org. Chem. 20 (1985) 5696-5704. (b) C.H. Behrens, S.Y. Ko, K.B. Sharpless, F.J. Walker, Selective transformation of 2,3-epoxy alcohols

and related derivatives. Strategies for nucleophilic attack at carbon-1, Org. Chem. 50 (1985) 5687-5696.

[5] (a) M. Chini, P. Crotti, E. Giovani, F. Macchia, M. Pineschi, Stereo-and regioselective metal salt-promoted ring opening of 1, 2-epoxides with thiols in acetonitrile, Synlett, 4 (1992) 303-305;(b) N. Iranpoor, I.M. Baltork, F.S. Zardalao, Ceric ammonium nitrate, an efficient catalyst for mild and selective opening of epoxides in the presence of water thiols and acetic acid, Tetrahedron, 47 (1991) 9861-9866.

[6] (a) A.K. Maiti, P. Bhattacharyya, Polyethylene glycol (PEG) 4000 catalysed regioselective nucleophilic ring opening of oxiranes - A new and convenient synthesis of β-hydroxy sulfone and β-hydroxy sulfide, Tatrahedron, 50 (1994) 10483-10490; (b) P. Raubo, J. Wicha, Pol. Regioselective ring opening of epoxides with thiols in water J. Chem. 69 (1995) 78.

[7] D.M. Hodgson, P.J. Comina, M.G.B. Drew. Chromium(II)-mediated synthesis of vinylbis(silanes) from aldehydes and a study of acid-and base-induced reactions of the derived epoxybis(silanes): a synthesis of acylsilanes, J. Chem. Soc. Perkin Trans 1 (1997) 2279-2289.

[8] P.F. Hudrlik, D. Ma, R.S. Bhamidipati, A.M. Hudrlik, Ring-Opening Reactions of α,β-Epoxy Silanes with Organocopper Reagents: Reaction at Carbon or Silicon?, J. Org. Chem. 61 (1996) 8655-8658.

[9] R. Boukherroub, G. Manuel, Unprecedented effects of the trimethylsilyl group on the reactivity of 3C-silylated silacyclopentenes and their derivatives, J. Organomet. Chem. 604 (2000) 141-149.

[10] K.D. Safa, F. Behmagham, KH. Ghorbanpour, Acid-catalyzed reactions of (3-(naphthalen-2-yl)-2,2-bis(trimethylsilyl)oxiran. A new synthesis of functional-group-substituted vinylsilanes, J. Org. Chem. 696 (2011) 1840-1844.

[11] M.J. Frisch, G.W. Trucks, H.B. Schlegel, et al., Gaussian 03, Revision 0.02, Gaussian, Inc., Wallingford CT, (2004).

[12] R. Ditchfield, Self-consistent perturbation theory of diamagnetism, Mol. Phys., 27 (1974) 789-807.

[13] R.I.I. Dennington, T. Keith, J. Millam, GaussView Version 4.1.2, Semichem Inc., Shawnee Mission, KS, (2007).

[14] N.M. OBoyle, A.L. Tenderholt, K.M. Langner, cclib: A library for package-independent computational chemistry algorithms, J. Comput. Chem, 29 (2008) 839-845.

[15] R.G. Baughman, S.L. Baldwin, Structure of the charge-transfer complexes 2,4,5,7-tetranitro-9-fluorenone-1-ethylnaphthalene (1/1) (I) and 2,4,5,7-tetranitro-9-fluorenone-3,6-dimethylphenanthrene (1/1) (II), Acta Crystallographica Section C Crystal Structure Communications, 49 (1993) 1840-1844.

[16] S. Kannan, A. Usman, H.K. Fun, meso-Bis (phenylsulfinyl) methane, Acta Cryst., C59 (2003) 268-270.

[17] P.R. Meehan, R.M. Gregson, C. Glidewell, G. Ferguson, Bis (4-methoxyphenylsulfonyl) methane: a Three-Dimensional Network Generated by Short C—H··· O Hydrogen Bonds, Acta Cryst, C53 (1997) 1975-1978.

[18] V.K. Rastogi, M.A. Palafox, R.P. Tanwar, L. Mittal, 3, 5-Difluorobenzonitrile: ab initio calculations, FTIR and Raman spectra, Spectrochimica. Acta., A58 (2002) 1987-2004.

[19] R.M. Silverstein, G.C. Basseler, T.C. Morill, Spectrometric Identification of Organic Compounds, 4th ed. New York: John Wiley and Sons, QD272 (1981) S6 S55.

[20] G.K. Hamer, I.R. Peat, W.F. Reynolds, Investigations of Substituent Effects by Nuclear Magnetic Resonance Spectroscopy and All-valence Electron Molecular Orbital Calculations. I, 4-Substituted Styrenes, Can. J. Chem., 51 (1973) 897-914.

[21] P. Politzer, D.G. Truhlar (Eds.), Chemical Application of Atomic and Molecular Electrostatic Potentials, Plenum, New York, (1981).

[22] ChemBioDraw Ultra, version 11.0 available from Cambridge Soft.

[23] ACD/HNMR and ACD/CNMR; Advanced Chemistry Development, Inc.: http://www.acdlabs.com.*Chem. Soc. Rev.,* 41 (2012) 3140-3152.

How to Cite This Article

Farnaz Behmagham; Zahra Asadi; Yahya Jamal Sadeghi. "Synthesis, spectroscopic and computational investigation of bis (3-methoxyphenylthio) ethyl) naphthalene". Chemical Review and Letters, 1, 2, 2018, 68-76. doi: 10.22034/crl.2018.85210